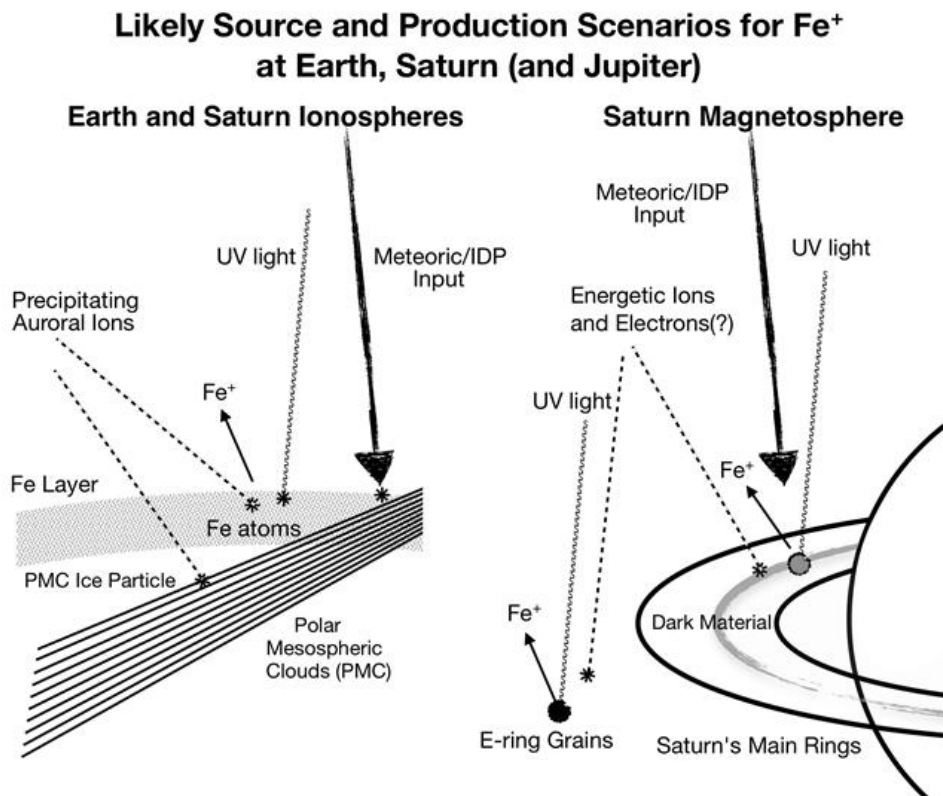


## POSSIBLE SOURCES - MOST LIKELY

Fe<sup>+</sup> In And Near Planetary Magnetospheres • AGU Fall Meeting • Christon et al. (2020)

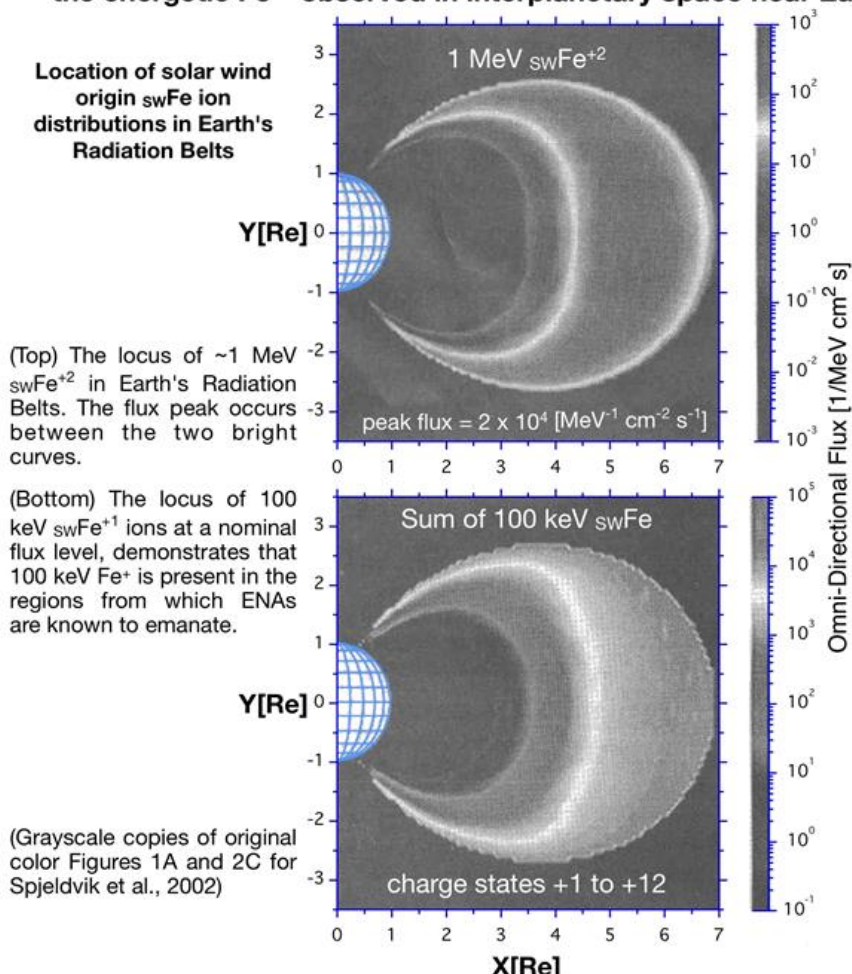


Meteoric particles and interplanetary-dust (IDP) bombard and ablate in planets' magnetospheres and thermospheres. These processes produce Fe atoms, Fe-containing icy particles, and compounds from which singly-ionized Fe, Fe<sup>+1</sup> ( $\equiv$ Fe<sup>+</sup>), can result when impacted by precipitating auroral particles or irradiated by solar UV. That Fe<sup>+1</sup> often becomes an integral part of their ionospheres (Plane, 2012; Frankland & Plane, 2015; Christon et al., 2015; 2017, and references therein). The resulting Fe<sup>+1</sup> can then participate in the outward transport processes from the upper ionosphere into the magnetosphere. The same overall processes involving precipitating energetic particle impact and meteoric bombardment/ablation likely occur in all planets' thermospheres, rings, and ring atmospheres. To our knowledge though, no set of observations has yet provided detailed measurement and identification of the specific acceleration mechanisms involved in these processes for Fe<sup>+1</sup> in any magnetosphere.

## POSSIBLE SOURCES - NEXT MOST LIKELY

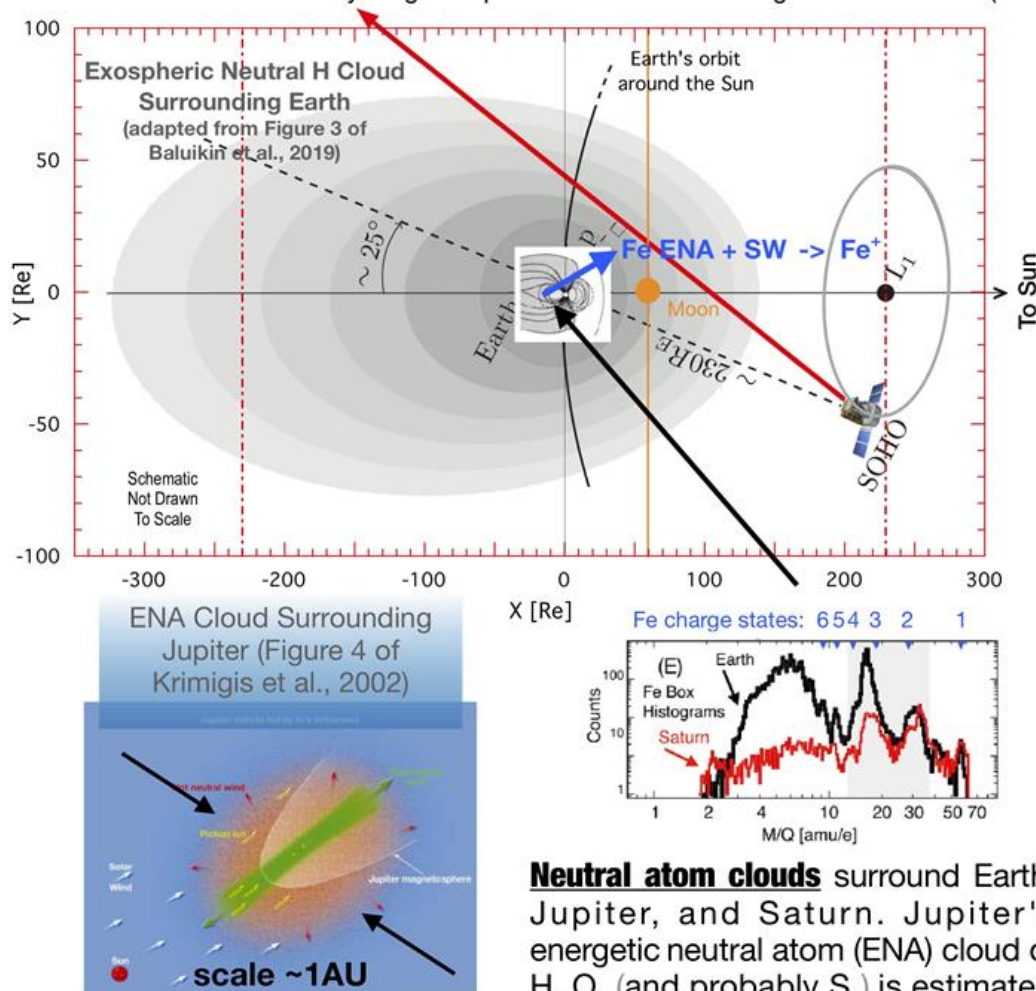
Fe<sup>+</sup> In And Near Planetary Magnetospheres • AGU Fall Meeting • Christon et al. (2020)

### The Solar Wind is Another Possible Source of Fe<sup>+</sup> at Earth Solar wind origin swFe<sup>(+6:+15)</sup> processed near-Earth may contribute to the energetic Fe<sup>+</sup> observed in interplanetary space near Earth.



Solar Wind origin Fe, swFe, ion fluxes in Earth's radiation belts were calculated using a data-based swFe<sup>+12</sup> input spectrum (Spjeldvik et al., 2002; Spjeldvik, 1996). (bottom) These distributions include swFe<sup>+1:5</sup>. ~100 keV Energetic Neutral Atoms, ENAs, are produced locally at < 7 R<sub>E</sub> from charge exchange (Brandt et al., 2002) - energies comparable to those of Fe<sup>+</sup> observed outside Earth's magnetosphere (Christon et al., 2017). ENAs may be lost from the magnetosphere continually, or, at minimum, during disturbed magnetospheric intervals.

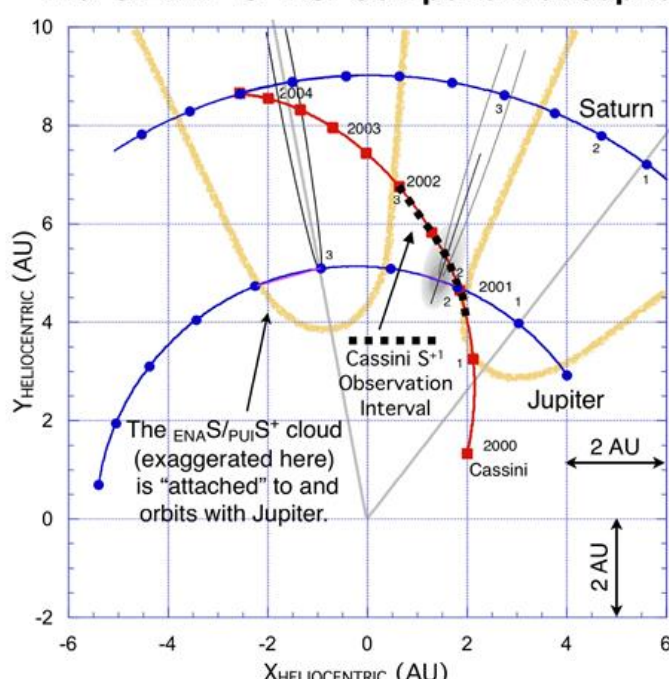
Fe<sup>+</sup> In And Near Planetary Magnetospheres • AGU Fall Meeting • Christon et al. (2020)



**Neutral atom clouds** surround Earth, Jupiter, and Saturn. Jupiter's energetic neutral atom (ENA) cloud of H, O, (and probably S), is estimated to be ~1AU (Krimigis et al., 2002). The recently discovered exospheric H cloud that surrounds Earth and extends to ~100 Re sunward of Earth, encompasses the Moon's orbit (Baluikin et al., 2019). If Earth has an ENA Fe component (sourced by solar wind Fe ions transported into the Radiation Belt), the resulting pickup Fe<sup>+</sup> ion flux in the solar wind might account for some of the Fe<sup>+</sup> observed by Geotail between Earth and the moon. No Fe<sup>+</sup> was observed near the Moon using a nearly identical ion spectrometer on Wind (Mall et al., 1998; Kirsch et al., 1998), so it might be that any of Earth's Fe ENAs are quickly ionized and picked up by the solar wind, never reaching the Moon.

Fe<sup>+</sup> In And Near Planetary Magnetospheres • AGU Fall Meeting • Christon et al. (2020)

### The S ENA - S<sup>+</sup> PUI Component at Jupiter

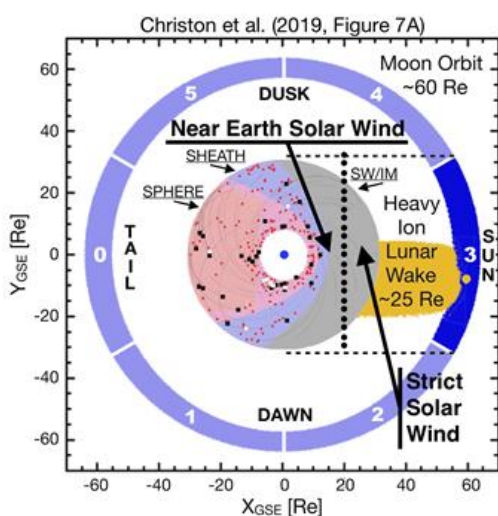
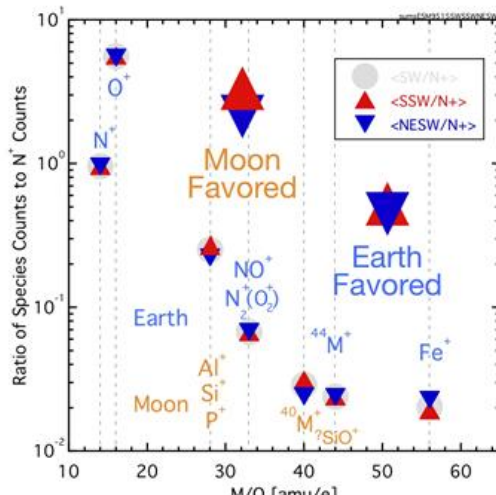
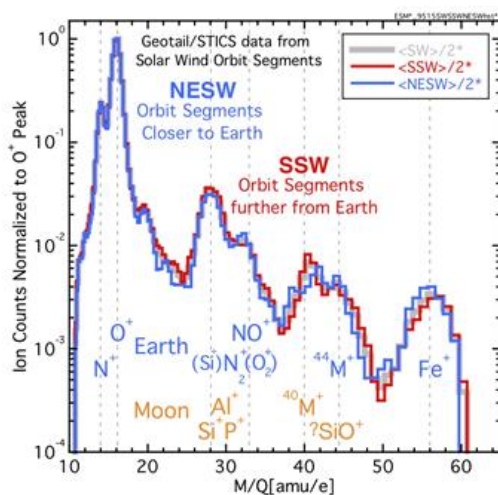


A sketch of Cassini's trajectory and Jupiter and Saturn orbits in heliocentric solar ecliptic coordinates. Shown at the start of each year, blue circles identify planets and red squares show Cassini spacecraft locations from 2000 to 2004. Cassini colocalizes with Saturn after mid-2004. Three common Jupiter's H, O, and S ENA/PUI cloud (e.g., Krimigis et al., 2002) is drawn both (1) exaggerated, as golden hyperbolae (radius of curvature ~1.4 AU), and (2) using a scaled image of Earth's neutral H cloud, width ~0.75 AU. Jovian origin S<sup>+</sup>, detected along the heavy, black-dashed trace (Christon et al., 2020), are likely pickup ions, PUI S<sup>+</sup>, expected from Jupiter's energetic neutral atoms, ENAS (Gruntman, 1997; Luhmann, 2003). As some of the S<sup>+</sup> can travel along the IMF to the point of observation from the cloud, the cloud's nominal size is probably somewhere between these estimates.

# UNLIKELY SOURCE CANDIDATES

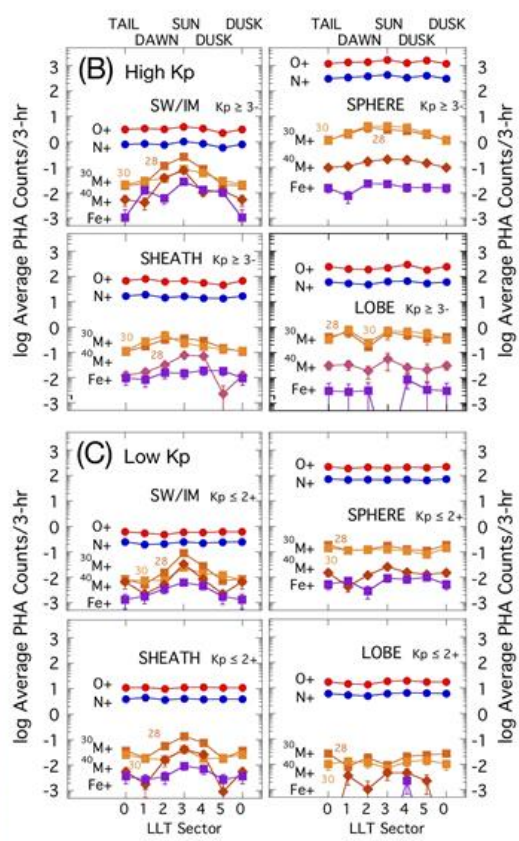
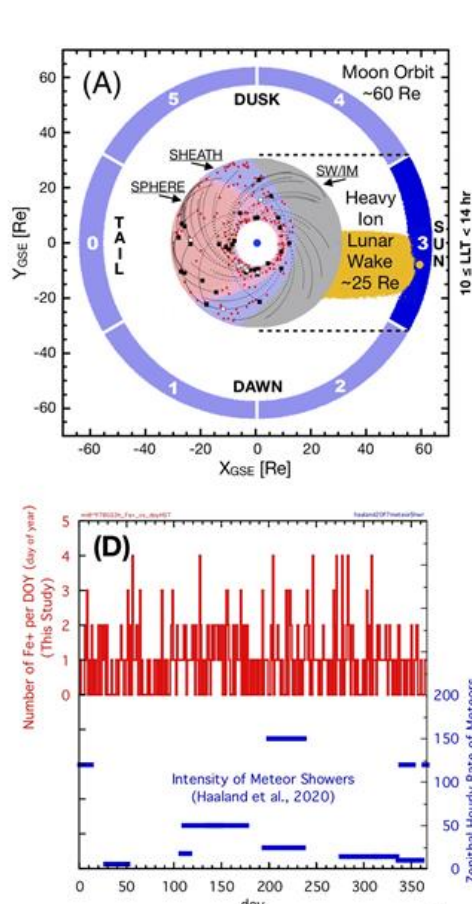
Fe<sup>+</sup> In And Near Planetary Magnetospheres • AGU Fall Meeting • Christon et al. (2020)

## The Main Source of Fe<sup>+</sup> is Most Likely Earth, Not the Moon



(top panels) Geotail/STICS solar wind, SW, data are separated into near-Earth solar wind, **NESW**, and strict solar wind, **SSW**, groups (left), ordered by M/Q and summed into relevant groups. In the NESW, at X<sub>GSE</sub> < 20 Re, Earth origin ion species counts are slightly higher than those of lunar origin ion species and vice-versa, lunar origin ion species counts are slightly higher than terrestrial origin ion species in the SSW at X<sub>GSE</sub> ≥ 20 Re.

Fe<sup>+</sup> In And Near Planetary Magnetospheres • AGU Fall Meeting • Christon et al. (2020)



### Fe<sup>+</sup> Occurrence Rates Compared to Lunar Orbital Location and Meteor Showers

(A, B, C) Panels from Figure 7 of Christon et al. (2020) show heavy ion occurrence rates collected in six equal Lunar Local Time (LLT) sectors in the ~80-200 keV/e range. When measured in the solar wind/interplanetary medium, SW/IM, the heavier ions shown are expected to exhibit higher SW convection-peaking centered in LLT = 3. Lunar ions (<sup>30</sup>M<sup>+</sup> and <sup>40</sup>M<sup>+</sup>) exhibit pronounced peaks centered on LLT = 3. Fe<sup>+</sup> exhibits a broad LLT = 3 centered enhancement in the SW/IM during high and low Kp intervals, not necessarily consistent with a lunar source. (D) The Fe<sup>+</sup> DOY-occurrence rate shows little relation to that of meteor showers listed by Haaland et al. (2020). Neither comparison supports an argument that Fe<sup>+</sup> occurrence depends on these factors.

# SUMMARY AND REFERENCES

## Summary

Fe<sup>+</sup> is clearly observed at Earth and Saturn, but has not yet been detected at Jupiter

Although clearly observed inside Saturn's magnetosphere, Fe<sup>+</sup> was not detected outside it

Although rare, Fe<sup>+</sup> is observed in all near-Earth (~9-35 R<sub>E</sub>) plasma regimes

Fe<sup>+</sup> occurrence times show little relation to lunar orbital location/timing and/or to meteor shower occurrence

Fe<sup>+</sup> production likely results from UV irradiation, auroral precipitating particles, and meteoric/IDP bombardment of and ablation in the thermospheres at Earth, Saturn, and Jupiter - as well as in other outer planet's thermospheres, rings, and ring atmospheres

High-charge-state (+6:+15) solar wind origin iron, SWFe, processed in Earth's radiation belts may result in Fe ENAs which are then ionized and picked-up by the solar wind, becoming or contributing to the energetic Fe<sup>+</sup> observed in interplanetary space near Earth. Such a Fe/Fe<sup>+</sup> ENA/PUI cloud would be smaller than the H/H<sup>+</sup> ENA/PUI cloud

Fe<sup>+</sup> is likely not the only ion observed at M/Q > 50 amu/e at Saturn

At Earth, our data show that the main source of Fe<sup>+</sup> is most likely Earth, not the Moon

Data: • Cassini/MIMI/CHEMS data are at <http://pds.nasa.gov>. • Geotail/EPIC/STICS data are at [http://spdf.gsfc.nasa.gov/pub/data/geotail/epic/stics\\_pha\\_ascii\\_gzip](http://spdf.gsfc.nasa.gov/pub/data/geotail/epic/stics_pha_ascii_gzip) and the JHU/APL Space Department.

## References

Baliukin, I. I., Bertaux, J. L., Quémerais, E., Izmodenov, V. V., & Schmidt, W. (2019). SWAN/SOHO Lyman- $\alpha$  mapping: The hydrogen geocorona extends well beyond the Moon. *Journal of Geophysical Research: Space Physics*, *124*, 861–885. <https://doi.org/10.1029/2018JA026136>

Brandt, P.C., R. Demajistre, E. C. Roelof, S. Ohtani, D. G. Mitchell, and S. Mende, IMAGE/high-energy energetic neutral atom: Global energetic neutral atom imaging of the plasma sheet and ring current during substorms, *J. Geophys. Res.*, *107*(A12), 1454, <https://doi.org/10.1029/2002JA009307>, 2002.

Christon, S. P., Hamilton, D. C., Gloeckler, G., Eastman, T. E., & Ipavich, F. M. (1994). High charge state carbon and oxygen ions in Earth's equatorial quasi-trapping region. *Journal of Geophysical Research: Space Physics*, *99*(A7), 13465–13488. <https://doi.org/10.1029/93JA0332>

Christon, S. P., D. C. Hamilton, J. M. C. Plane, D. G. Mitchell, R. D. DiFabio, & S. M. Krimigis (2015). Discovery of suprathermal Fe<sup>+</sup> in Saturn's magnetosphere. *Journal of Geophysical Research: Space Physics*, *120*. <https://doi.org/10.1002/2014JA020906>

Christon, S. P., Hamilton, D. C., Plane, J. M. C., Mitchell, D. G., Grebowsky, J. M., Spjeldvik, W. N., & Nylund, S. R. (2017). Discovery of suprathermal ionospheric origin Fe<sup>+</sup> in and near Earth's magnetosphere. *Journal of Geophysical Research: Space Physics*, *122*. <https://doi.org/10.1002/2017JA024414>

Christon, S. P., Hamilton, D. C., Mitchell, D. G., Plane, J. M. C., & Nylund, S. R. (2020). Suprathermal magnetospheric atomic and molecular heavy ions at and near Earth, Jupiter, and Saturn: Observations and identification. *Journal of Geophysical Research: Space Physics*, *125*. <https://doi.org/10.1029/2019JA027271>

(Christon et al., 2020, this work: Poster, AGU Fall 2020; PDF, Contact 1st Author).

Frankland, V. L. & J. M. C. Plane (2015). Fe embedded in ice: the impacts of sublimation and energetic particle bombardment. *Journal of Atmospheric and Solar-Terrestrial Physics*, *127*, 103-110. <https://doi.org/10.1016/j.jastp.2014.12.004>

Gruntman, M. (1997). Energetic neutral atom imaging of space plasmas. *Review of Scientific Instruments*, *68*, 3617-3656. <https://doi.org/10.1063/1.1148389>

Haaland, S., Daly, P. W., Vilenius, E., Krcelic, P., & Dandouras, I. (2020). Suprathermal Fe in the Earth's plasma environment: Cluster RAPID observations. *Journal of Geophysical Research: Space Physics*, *125*, e2019JA027596. <https://doi.org/10.1029/2019JA027596>

Kirsch, E., Wilken, B., Gloeckler, G., Galvin, A. B., Geiss, J., & Hovestadt, D. (1998). Search for lunar pickup ions, *COSPAR Colloquia Series* (Vol. 9, pp. 65–69). Beijing: Pergamon. [https://doi.org/10.1016/S0964-2749\(98\)80011-5](https://doi.org/10.1016/S0964-2749(98)80011-5)

Krimigis, S. M., Mitchell, D. G., Hamilton, D. C., Dandouras, J., Armstrong, T. P., Bolton, S. J., et al. (2002). A nebula of gases from Io surrounding Jupiter. *Nature*, *415*(6875), 994–996. <https://doi.org/10.1038/415994a>

Luhmann, J. G. (2003). Expected heliospheric attributes of Jovian pickup ions from the extended neutral gas disk. *Planetary and Space Science*, *51*, 387–392. [https://doi.org/10.1016/S0032-0633\(03\)00034-5](https://doi.org/10.1016/S0032-0633(03)00034-5)

Mall, U., Kirsch, E., Cierpka, K., Wilken, B., Soding, A., Neubauer, F., et al. (1998). Direct observation of lunar pick-up ions near the Moon. *Geophysical Research Letters*, *25*, 3799–3802. <https://doi.org/10.1029/1998GL900003>

Plane, J. M. C. (2012). Cosmic dust in the Earth's atmosphere. *Chemical Society Review*, *41*, 6507–6518. <https://doi.org/10.1039/C2CS35132C>

Postberg, F., Clark, R. N., Hansen, C., Coates, A., Daile Ore, C. M., Scipioni, F., et al. (2018). Plume and surface composition of Enceladus. In P. M. Schenk, et al. (Eds.), *Enceladus and the icy moons of Saturn* (129–162). Tucson, AZ: University of Arizona. [https://doi.org/10.2458/azu\\_uapress\\_9780816537075-ch007](https://doi.org/10.2458/azu_uapress_9780816537075-ch007)

Spjeldvik, W. N., Bourdarie, S., & Boschen, D. (2002). Solar origin iron ions in the Earth's radiation belts: Multi-dimensional equilibrium configuration modeling with charge states 1 through 12. *Advances in Space Research*, *30*(12), 2835–2838. [https://doi.org/10.1016/S0273-1177\(02\)80426-4](https://doi.org/10.1016/S0273-1177(02)80426-4)

Spjeldvik, W. N. (1996). Numerical modeling of stably and transiently confined energetic heavy ion radiation in the Earth's magnetosphere. *Radiation Measurements*, *26*(3), 309–320. [https://doi.org/10.1016/1350-4487\(96\)00059-5](https://doi.org/10.1016/1350-4487(96)00059-5)